

Aus der Klinik für Zahnärztliche Prothetik, Propädeutik und Werkstoffkunde
(Direktor: Prof. Dr. M. Kern)
im Universitätsklinikum Schleswig-Holstein, Campus Kiel
am der Christian-Albrechts-Universität zu Kiel

**Effect of changes in sintering parameters on physical
properties of monolithic translucent zirconia**

Inauguraldissertation zur
Erlangung der Würde eines Doktors der Zahnheilkunde der
Medizinischen Fakultät
der Christian-Albrechts-Universität zu Kiel

vorgelegt von
Kamal Khaled Ebeid Ahmed
aus Kairo, Ägypten
Kiel 2015

1. Berichterstatter: Prof. Dr. M. Kern

2. Berichterstatter: Prof. Dr. Dr. I.Springer

Tag der mündlichen Prüfung: 14-11-2016

Zum Druck genehmigt, Kiel, den 15-11-2016

Gez: _____

Index

1.	List of abbreviations	1
2.	Introduction.....	2
2.1.	Zirconia restorations	2
2.2.	Color and translucency.....	5
2.3.	Surface roughness.....	6
2.4.	Phase transformation.....	6
2.5.	Biaxial flexural strength.....	7
2.6.	Surface hardness.....	8
3.	Purpose of the study	9
4.	Materials and Methods	10
4.1.	Fabrication of zirconia discs.....	12
4.2.	Color reproduction and translucency	17
4.3.	Surface roughness.....	19
4.4.	Microstructure analysis	20
4.5.	Biaxial flexural strength.....	22
4.6.	Vickers hardness test.....	23
4.7.	Data management and analysis	25
5.	Results.....	26
5.1.	Color reproduction.....	26
5.2.	Translucency.....	28
5.3.	Surface roughness.....	30
5.4.	Microstructure analysis	31
5.5.	Biaxial flexural strength.....	32
5.6.	Surface hardness.....	33
6.	Discussion.....	34
6.1.	Discussion of methodology	34
6.2.	Discussion of results	35
7.	Conclusions.....	38
8.	Summary	39
9.	References.....	43

1. List of abbreviations

ΔE: Delta E

BFS: Biaxial flexural strength

CAD: Computer aided design

CAM: Computer aided manufacturing

CR: Contrast ratio

FDP: Fixed dental prosthesis

Ra: Surface roughness

TP: Translucency parameter

VHN: Vickers hardness number

XRD: X-ray diffraction

ZrO₂: Zirconium dioxide

2. Introduction

2.1. Zirconia restorations

The increased popularity of all-ceramic materials as an alternative to metal-ceramic restorations is attributable to their excellent aesthetics, chemical stability and biocompatibility. However, the brittleness and low tensile strength of conventional glass-ceramics limit their long-term clinical application in restorations.^[4] Several glass-ceramics have been introduced such as high alumina-content glass-infiltrated ceramic core material (In-Ceram Alumina) and lithium disilicate glass-ceramic (e.max press) which has been successfully used for crowns,^[52] anterior fixed dental prostheses (FDPs) and three-unit FDPs replacing the first premolar. However, these materials do not have sufficient strength to allow reliable use for FDPs, especially in the molar region.^[73]

Recently, the development of advanced dental ceramics has led to the application of partially stabilized zirconia in restorative dentistry which can be produced using computer aided design/computer-aided manufacture (CAD/CAM) systems. The use of zirconia-based ceramics for dental restorations has risen in popularity due to their superior fracture strength and toughness compared with other dental ceramic systems.^[28, 79, 80] Zirconium dioxide (ZrO_2), known as zirconia is a white crystalline oxide of zirconium. Although pure zirconium oxide does not exist in nature, it is found in the mineral baddeleyite or zircon.^[83]

The research and development on zirconia as a biomaterial started in the late sixties of the last century. The first paper concerning biomedical application of zirconia was published in 1969 by Helmer and Driskell,^[32] while the first paper concerning the use of zirconia to manufacture ball heads for total hip replacements, which is the current main application of this ceramic biomaterial, was introduced by Christel et al. in 1988.^[18]

Zirconia is a polycrystalline ceramic without any glass component. Being polymorphic, three forms of zirconia exist: monoclinic, cubic and tetragonal. Pure zirconia assumes the monoclinic form at room temperature which is stable up to 1,170°C. Beyond this temperature, a transformation to the tetragonal phase occurs, which is stable up to 2,370°C, after which the cubic phase transformation is seen. A transformation of tetragonal to monoclinic occurs while cooling down to the temperature of 1,170°C. This is associated with a volume expansion of 3% to 5%.^[62]

Addition of stabilizing oxides such as calcium oxide, magnesium oxide, cerium oxide and yttrium oxide stabilizes zirconia in its tetragonal phase at room temperature. Tensile

Introduction

stresses at a crack tip will cause the tetragonal phase to transform into the monoclinic phase with an associated 3-5% localized expansion. This volume increase creates compressive stresses at the crack tip that counteract the external tensile stresses and retards crack propagation. This phenomenon is known as transformation toughening.^[7]

Zirconia-based restorations have become very popular due to their superior mechanical properties with flexural strength more than 1,000 MPa and excellent biocompatibility. Due to their high opacity zirconia core is usually veneered with veneering porcelain. However, in clinical service, the most frequent failure is the chipping of the veneer, while the high-strength zirconia substructure is mostly not affected.^[54, 63, 65, 66, 69, 83] In specific clinical situations, such as when the occlusal or palatal space is limited or in cases where a patient's parafunctional activity (e.g., bruxism) may contraindicate this veneering application the use of unveneered zirconia ceramic seems to be an option for all-ceramic restorations.^[26]

A new innovative possibility for dental restorations is the construction of monolithic ceramic restorations without veneering. These restorative solutions have no porcelain overlay material to risk shear or fracture, nor do they require specialized pressing techniques and equipment.^[48] Fabricating mono-block restorations from pure zirconia could increase the mechanical stability and expand the range of indications. However, zirconia is known as a whitish, opaque core material. Optical appearance of opaque zirconia might be improved by modifications in the fabrication and sintering process, which were shown to increase translucency.^[42] The clinical advantage of these restorations is defined by significantly reduced material thickness in comparison to veneered zirconia restoration or other monolithic restorations. These restorations can be preshaded or colored prior to sintering, followed by characterization by staining thus good esthetic results in the posterior region can be achieved, even in cases with substantially reduced space.^[64, 68] Beuer et al. in 2012 reported that glazed full-contour zirconia crowns showed similar translucency, contact wear of the restoration and contact wear at antagonist as veneered zirconia crowns. However, glazed full-contour zirconia crowns showed higher fracture loads than veneered zirconia crowns.^[11]

Zirconia core materials are usually fabricated by milling technology.^[21] The restorations are processed either by soft machining of partially sintered blocks, followed by final sintering at high temperature or by hard machining of fully sintered blocks with a density of approximately 99.5% of the theoretical density.^[49, 78] Soft machining is much easier and prevents the stress induced transformation from tetragonal to

Introduction

monoclinic phase. However, the shrinkage during the additional sintering results in frameworks with less accurate marginal fit.^[45] Hard machining is technically more difficult, wears the machining hardware at a much higher rate, induces a significant amount of monoclinic zirconia, and may introduce micro cracks in the material that result in higher susceptibility to lower temperature degradation and lower reliability.^[49, 85] However, it offers higher precision since only 1-step sintering is sufficient.^[45]

Partially sintered frameworks are milled from porous blocks with incomplete sintered grains and open boundaries to larger dimensions and require further sintering for the ceramic to gain its full density.^[21, 76] This sintering procedure is accompanied by a sintering shrinkage of about 20% to 30%.^[50] In this stage heat is transmitted to the surface of the material and reaches its core by thermal conduction. The sintering cycle is divided into a heating stage, a holding stage at the final sintering temperature and a cooling stage.^[51] Alterations in this sintering cycle maybe used in order to optimize the properties of zirconia. However, several authors reported that although changes in the sintering parameters may optimize these properties they may also be detrimental to the material itself.^[83]

Stawarczyk et al. in 2013 studied the effect of sintering temperature on the biaxial flexural strength and contrast ratio of zirconia discs. Zirconia specimens were divided into nine groups according to the following sintering temperatures: 1,300°C, 1,350°C, 1,400°C, 1,450°C, 1,500°C, 1,550°C, 1,600°C, 1,650°C, and 1,700°C. They were sintered at a heating rate of 8°C/min and a holding time of 2 hours. Results showed that the highest flexural strength was obtained with temperatures between 1,400°C and 1,550°C. They also concluded that above 1,550°C a decrease in flexural strength will occur due to migration of yttrium to the grain boundaries. In a similar study, Hjerpe et al. evaluated the effect of shortening the sintering cycle by increasing the heating rate and lowering the sintering holding time the flexural strength of zirconia core material. However, they concluded that this had no effect on the strength of zirconia. ^[35,75]

Several authors had also tried to enhance translucency of zirconia core material using changes in the sintering parameters. They all reached the conclusion that increasing either the sintering time or the sintering temperature will lead to better translucency.^[42, 44]

Recently translucent zirconia was introduced which allows the use of full contour zirconia restorations without the need for any veneering ceramic. These restorations were able to attract increasing attention because of their unique combination of optical and mechanical properties.^[90] It is manufactured either by decreasing the grain size to less than 500 nm, eliminating light scattering alumina sintering aids, or by incorporating zirconia

crystal in the cubic phase.^[89, 91]

2.2. Color and translucency

An objective method of evaluating color differences requires an ordered system for the classification of color, as well as equipment capable of quantifying color differences. The use of colorimetric measurements provides interpretation of subjective evaluations related to the perception of color as physical values.^[58]

The widely recognized CIE L*a*b* color order system, developed in 1978 by the Commission Internationale de l'Éclairage (International Commission on Illumination), is commonly used in dental research.^[22, 33] This system defines color in terms of 3 coordinate values (L*, a*, and b*), which locate the color of an object within a 3-dimensional color space. The L* coordinate represents the brightness of an object represented on the y-axis, the a* value represents the red (positive x-axis) or green (negative x-axis) chroma, and the b* value represents the yellow (positive z-axis) or blue (negative z-axis) chroma. The color difference (ΔE) between 2 objects, or in the same object before and after it is subjected to particular conditions, can be determined by comparing the differences between the respective coordinate values for each object or situation.^[22]

Translucency is defined as the relative amount of light transmission or diffuse reflectance from a substrate surface through a turbid medium. The translucency of dental ceramic has a close relationship with its chemical composite and microstructure.^[13] The chemical nature, the amount of crystals, the size of particles, the pores and the sintered density determine the amount of light that is absorbed, reflected, and transmitted. All of the above influence the optical property of core ceramics.^[31]

Multiple crystalline contents used to strengthen the ceramic reduce the translucency because of the different refractive indices and the inhomogeneity of crystals. Since Y-TZP consists of polycrystals and has a different refractive index to the matrix, most of the light passing through it is intensively scattered and diffusely reflected, leading to opaque appearance. So the translucency of zirconia core ceramic is commonly lower than that of spinell, alumina, and feldspathic porcelains. In view of the esthetic drawbacks of zirconia, researchers have worked on optimizing production conditions to improve the optical property.^[31]

There are several methods to evaluate translucency and opacity of aesthetic restorative materials, such as: direct transmittance of light, the contrast ratio (CR) and the translucency parameter (TP).^[47, 53]

Factors affecting translucency of zirconia

- A- Thickness of the material [8,38]
- B- Type of zirconia [8,44]
- C- Shade of zirconia [74]
- D- Sintering conditions [42,44,75]

2.3. Surface roughness

Surface roughness (Ra), often shortened to roughness, is a measure of the texture of a surface. It is quantified by the vertical deviations of a real surface from its ideal form. If these deviations are large, the surface is rough; if they are small the surface is smooth. Roughness is typically considered to be the high frequency, short wavelength component of a measured surface. It plays an important role in determining how a real object will interact with its environment. Rough surfaces usually wear more quickly and have higher friction coefficients than smooth surfaces. Roughness is often a good predictor of the performance of a mechanical component, since irregularities in the surface may form nucleation sites for cracks or corrosion, on the other hand, roughness may promote adhesion.^[5, 17, 30] Many anatomically contoured zirconia crowns are glazed and stained superficially during fabrication to improve their esthetic properties.^[92] At insertion, the occlusal adjustment of ceramic crowns may roughen the occluding surface, the adjusted area of which will require polishing. A previous in vitro study has reported that polishing ceramic materials decreases their roughness and decreases opposing enamel wear.^[56] Additionally, polished ceramics produce less wear of opposing enamel than glazed ceramics. A possible explanation is that the glazed surface is quickly worn away to reveal the rough surface of unpolished ceramic beneath. Therefore, polishing ceramics before glazing may help prevent opposing enamel wear.^[23]

Factors affecting surface roughness of zirconia

- A- Milling technique [85]
- B- Surface treatment performed [14,20,57]
- C- Finishing procedure [41,68,82]

2.4. Phase transformation

The quantitative analysis of ZrO₂ systems with monoclinic, tetragonal, and cubic polymorphs has been of interest since the study on the martensitic nature of monoclinic-tetragonal transformation and is of special importance in the research area of the zirconia transformation toughening. The intensity ratio of the reflections of two phases has always

been used for the quantitative analysis by X-ray diffraction. Plotted calibration curves were used to calculate the volume fraction of monoclinic phase by the equations described by Garvie, Nicholson, and Toraya.^[25,81] Usually new commercial zirconia has only tetragonal crystals and no monoclinic portion.^[21]

2.5. Biaxial flexural strength

Mechanical properties such as strength are the first parameters to be assessed to understand the clinical potential and limitations of a dental ceramic.^[29] Flexural strength is generally considered a meaningful and reliable method to assess the strength of brittle materials as they are much weaker in tension than in compression. In addition, the strength reliability and variability of materials should be studied as the failure stresses of brittle materials are statistically distributed as a function of the flaw size distribution in the material.^[12]

The flexural strength of a material is its ability to bend before it breaks.^[4] Flexural forces are the result of masticatory forces generated in clinical situations where dental materials need to withstand repeated flexing, bending, and twisting. Materials with high flexural strength provide restorations with less susceptibility to bulk fracture.^[86]

According to the ISO 6872 standards for testing ceramic materials, a monolayered disc specimen is positioned in the sample holder on top of the three supporting balls. The load at fracture is recorded and the biaxial flexure strength for the specimen is calculated using the following equation^[1]:

$$S = [-0.2387P(X - Y)]/d^2$$

S: biaxial flexural strength (MPa); **P**: fracture load (N); **d**: specimen disk thickness at fracture origin (mm).

$$X: (1 + \nu) \ln(r2 / r3)^2 + [(1 - \nu) / 2] (r2 / r3)^2$$

$$Y: (1 + \nu) [1 + \ln(r1 / r3)^2] + (1 - \nu) (r1 / r3)^2$$

Where ν is Poisson's ratio, **r1** is the radius of the support circle, **r2** is the radius of the loaded area, and **r3** is the radius of the specimen.

Factors affecting the biaxial flexural strength of zirconia

- A- Type of zirconia ^[15, 72, 88]
- B- Surface treatment performed ^[39, 57, 60]
- C- Finishing procedure ^[60]
- D- Dipping time in coloring liquid ^[34]
- E- Aging ^[24]

2.6. Surface hardness

Hardness may be broadly defined as the resistance to permanent surface indentation or penetration. It is measured as a force per unit area of indentation. Based on its definition, hardness is a very important property of dental materials due to its direct correlation to ease of cutting, finishing, polishing and resistance to scratch of the material. One of the most common methods of testing hardness especially of ceramics is the Vickers hardness test which utilizes a square-based diamond indenter that is forced into the material with a definite load application.^[70]

3. Purpose of the study

Several authors had studied the effect of changing sintering parameters on regular zirconia core material. However, they only focused on the effect of these changes on the translucency and biaxial flexural strength of the material. With the introduction of monolithic translucent zirconia it is not known whether this material will be subjected to the similar changes as regular zirconia core material or not. None of the previous studies also determined the effect of these changes on the color reproduction of pre-shaded zirconia as they all dealt with un-shaded zirconia material.

Therefore the aim of this study was to determine the effect of changing the sintering temperature (1,460°, 1,530°, and 1,600°C) and the sintering holding time (1, 2 and 4 hours) on the color reproduction, translucency, surface roughness, microstructure, biaxial flexural strength, and surface hardness of monolithic translucent zirconia.

4. Materials and Methods

Materials

The material used in this study and its composition are presented in Table 1.

Table 1: Material used in this study

	Material	Brand	Composition	
1	Translucent zirconia blanks	Bruxzir™ shaded blanks, Glidewell, Frankfurt, Germany	Zirconium Oxide ZrO ₂	<89%
			Yttrium Oxide Y ₂ O ₃	>6%
			Hafnium Oxide HfO ₂	>4%
			Aluminum Oxide Al ₂ O ₃	>1%

The properties of the translucent shaded zirconia blanks are presented in Table 2

Table 2: Properties of shaded Bruxzir blanks as given by manufacturer

Properties	
Coefficient of thermal expansion (25-500°C)	10^{-6}K^{-1}
Flexural Strength	>1,000 MPa
Density	6.05 gm/cm ³
Fracture toughness	>8 MPa/m ^{1/2}

Methods

In this in-vitro study, monolithic translucent zirconia discs were constructed using CAD/CAM technology. They were later tested for several optical and mechanical properties after being sintered with different sintering parameters in a zirconia sintering furnace (Bruxzir FastFire, Glidewell, Frankfurt, Germany).

A total of 90 monolithic zirconia discs were fabricated. Specimens were divided into three main groups according to the sintering temperature as shown in Table 3:

Group 1: 1,460°C (30 specimens)

Group 2: 1,530°C (30 specimens)

Group 3: 1,600°C (30 specimens)

Each group was later subdivided according to the sintering holding time into three subgroups:

Subgroup a: 1 hour (10 specimens)

Subgroup b: 2 hours (10 specimens)

Subgroup c: 4 hours (10 specimens)

All specimens were sintered at a heating and cooling rate of 10°C.

Table 3: Experimental factorial design

Sintering Time (Hour) \ Sintering Temp (°Celsius)	Subgroup a 1 hour	Subgroup b 2 hours	Subgroup c 4 hours	Total
Group 1 1,460°C	1a n=10	1b n=10	1c n=10	30
Group 2 1,530°C	2a n=10	2b n=10	2c n=10	30
Group 3 1,600°C	3a n=10	3b n=10	3c n=10	30
Total	30	30	30	90

4.1. Fabrication of zirconia discs

a) Designing of the discs

Design of zirconia discs having 15 mm diameter and 1 mm thickness was performed by the CAD system software (Dental System 2.6, 3Shape A/S, Copenhagen, Denmark). There was no need to scan any template as the software was used to import the disc design from the standard template library. No adjustments were needed to the design imported. The shape of the disc was confirmed and exported to the CAM system (Fig. 1).

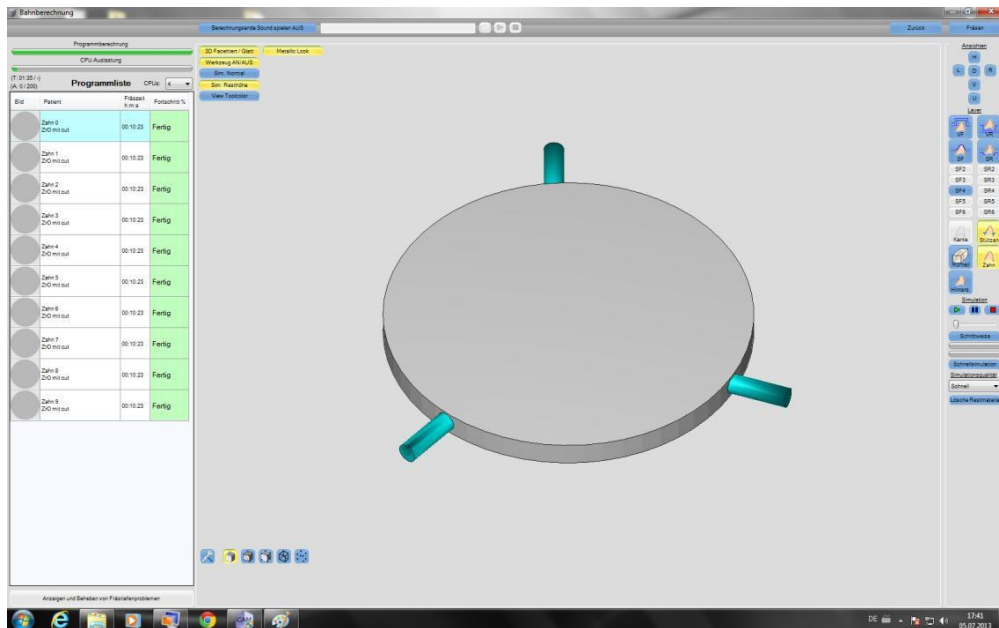


Figure 1: Imported disc design from standard template library

b) Milling of the discs

Milling of the discs was performed by a dental milling machine (Datron D5, Datron AG, Muhltal-Traisa, Germany) (Fig. 2) which is a five axis dental milling machine used for milling zirconium oxide, titanium, wax, composite, gypsum, and ceramics. As soon as the disc design was imported by the milling machine, a dialog box popped out to choose the type of material that will be milled and zirconia blanks were chosen.



Figure 2: Milling machine

Ten shaded translucent zirconia blanks were used in this study (Bruxzir, Glidewell, Frankfurt, Germany) (lot number: B265373). The blanks had a thickness of 12 mm and shade A3.

The blanks were inserted into the milling machine and discs were milled according to the design imported. The discs were milled with an approximate 20%-25% oversize. Each blank is labeled with a barcode and a specific enlargement factor to calculate the exact oversize needed during milling to compensate for the sintering shrinkage. The barcode was automatically read prior to milling each blank by the milling machine. The order to mill the discs was then given to the milling machine.

After the milling process finished the discs were still not separated from the main blank (Fig. 3). A specific Bruxzir finishing bur was used to separate the discs from the main blank. All discs were then put in an ultrasonic bath of distilled water for 10 minutes to remove any ZrO_2 residues.

Materials and methods

Disc specimens were then inserted in the drying unit (Robocam, Thermostar, Aachen, Germany) (Fig. 4) for 5 minutes at a temperature of 80°C to remove any liquid that penetrated after the cleaning process.



Figure 3: Close-up of blank after milling the discs



Figure 4: Drying unit

c) **Sintering of the zirconia discs**

After the drying process, the discs were randomly divided into 9 pre-determined subgroups. The discs were put into sintering boat which is made of pure alumina and a single layer of 2 mm zirconia sintering beads was put underneath the discs (Fig. 5).

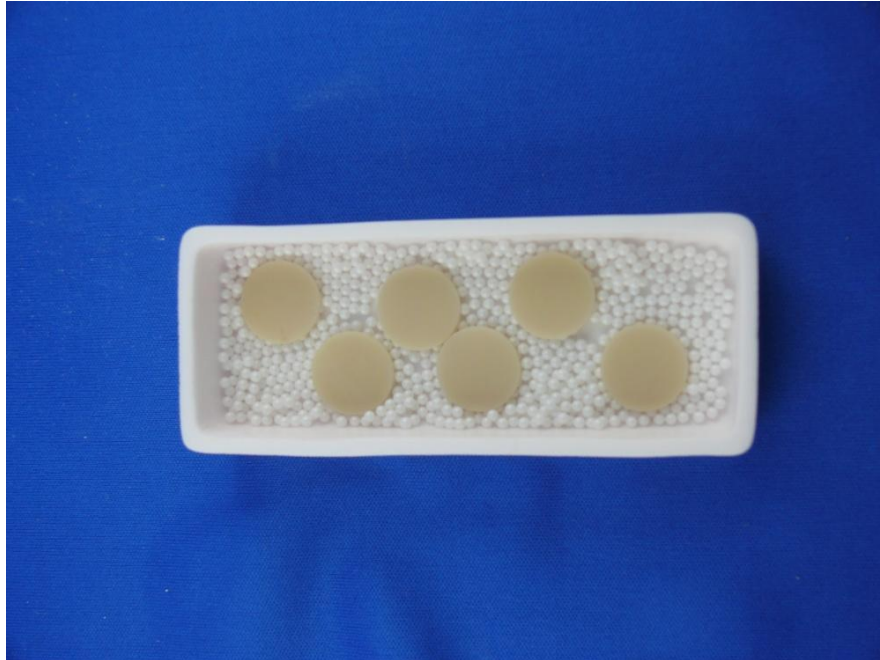


Figure 5: Sintering boat, beads and discs

The discs were then put into sintering furnace (Bruxzir Fastfire, Glidewell Bruxzir, Frankfurt, Germany) sintering furnace (Fig. 6) and sintered according to the predetermined sintering temperatures and times. Before sintering each subgroup, the sintering temperature and time were adjusted using the furnace's control panel and the heating and cooling rates were set to 10°C. Before the measurements were performed all specimens were ultrasonically cleaned in a solution of 99% isopropanol for 5 min then they were air dried for 10 seconds to remove any contamination from the manufacturing process.



Figure 6: Sintering furnace

4.2. Color reproduction and translucency

Color reproduction and translucency were measured for each specimen in each subgroup using a spectrophotometer (Vita Easyshade, Vita, Bad Säckingen, Germany) (Fig. 7). After each time the spectrophotometer was turned on it was calibrated in the calibration slot according to manufacturer's instructions to ensure accuracy of measurements.



Figure 7: Spectrophotometer

The spectrophotometer was set to the restoration mode and the shade A3 was selected. The spectrophotometer aperture was centralized on the center of each disc and given the order to measure its color. In this mode the spectrophotometer shows the difference between the selected shade and the measured shade (ΔE). Three measurements were taken for each specimen and their average was recorded. Mean ΔE values below 3.0 were considered “clinically imperceptible”, ΔE values between 3.0 and 5.0 were considered “clinically acceptable” and ΔE values above 5.0 were considered “clinically unacceptable”.^[3, 22]

For measuring translucency, the spectrophotometer was used to obtain a quantitative measurement of translucency by comparing reflectance of light through the test specimen over a backing with a white (CIE $L^*=96.7$, $a^*=0.1$, $b^*=0.2$) and black (CIE $L^*=10.4$, $a^*=0.4$, $b^*=0.6$) background (Fig. 8). For each specimen three measurements were taken and the average CIELAB coordinates were recorded. The contrast ratio (CR) for each specimen was calculated according to the following equations:

$$CR = Y_b/Y_w \text{ and } Y = [(L+16)/116]^3 \times 100$$

Where Y_b is the reflectance over a black background and Y_w is the reflectance over a white background. This ratio tends toward unity for opaque materials and toward zero for transparent materials.

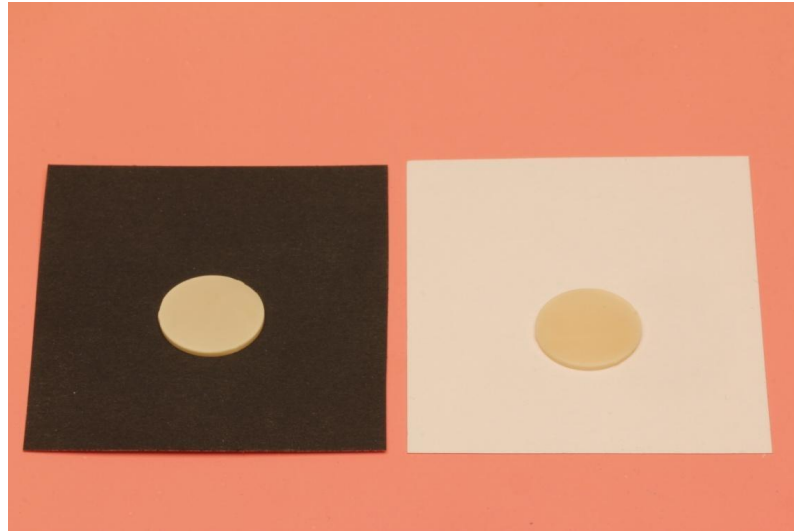


Figure 8: Specimens over black and white background

4.3. Surface roughness

All specimens were measured for surface roughness using a 3D laser scanning microscope (Keyence VX-100, Keyence, Neu-Isenburg, Germany) (Fig. 9).



Figure 9: 3D laser scanning microscope

Each specimen was centered on the microscope's platform and the whole surface of the discs was imaged using the microscope under 10× magnification to ensure that there were no surface scratches that could influence the measurement. An area at the exact center of the disc was specified (700 μm ×500 μm) and the magnification was raised to 100× (Fig. 10).

Materials and methods

The focus was adjusted automatically using the microscope's software and then the order of the scanning was given. After the microscope finished the scanning process a 3D surface image was produced. The VK analyzer software was later opened and the whole image was selected and measured for surface roughness. Two different areas above and below the center by 5 mm were later selected, scanned, and the average Ra for the three measurements was recorded.

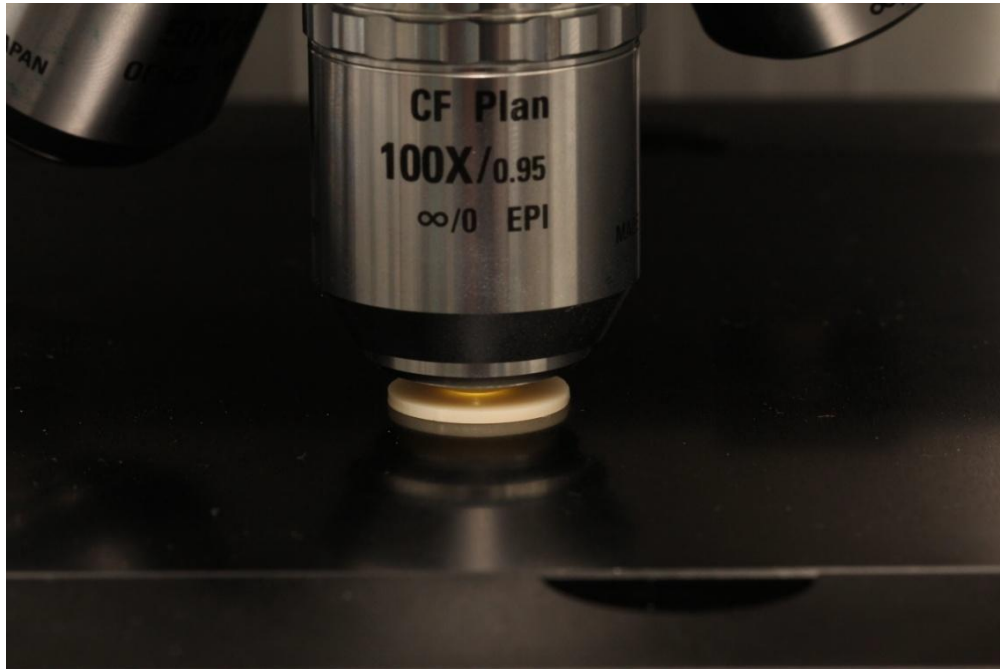


Figure 10: 100× magnification scanning lens

4.4. Microstructure analysis

Three samples from each subgroup were analyzed using an X-ray diffractometer (Seifert PTS-3000, General Electric, Connecticut, USA) for detection of the ZrO₂ tetragonal and monoclinic phases available. Each disc was centered in the sample holder and inserted in the diffractometer.

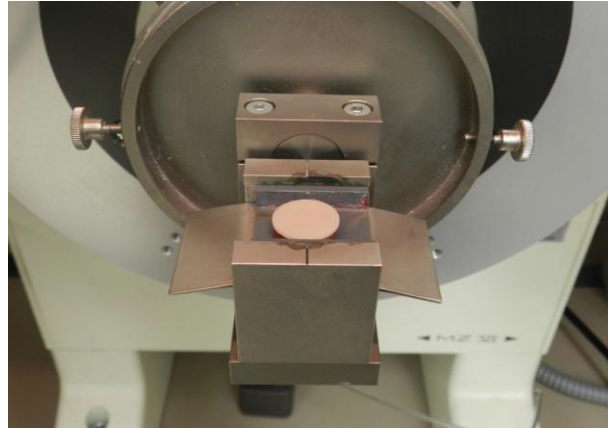


Figure 11: Zirconia disc placed in specimen holder

Specimens were placed so that the radiation beam was directed exactly at the center of the disc. Specimens were subjected to Cu K alpha radiation with a range of 20° - 40° , a step size of 0.02° and the scan time per step was 10 seconds (Figs. 11, 12). This radiation range selected covered the tetragonal and monoclinic crystalline phases of ZrO_2 . After each specimen was scanned the analyzer software was used to plot a graph between the incident radiation angle and the diffraction pattern. The graph obtained was used to analyze the crystalline phases available.

One sample from each subgroup was cleaned; dried, gold sputter coated and examined under $10,000\times$ magnification using a scanning electron microscope (XL 30 CP, Philips, Surrey, England) to calculate the average grain size using a base of at least 150 grains.



Figure 12: X-ray source, disc and receptor

4.5. Biaxial flexural strength

Specimens were tested for biaxial flexural strength (BFS) using piston-on-three ball technique in a universal testing machine (Zwick Z010, Zwick, Ulm, Germany) according to the ISO 6872 specifications for testing ceramic materials. A 10 mm diameter metallic platform was constructed, above which rested three 3.2 mm diameter steel balls that were equidistant from each other (Fig. 13).

Each disc was placed on the steel balls and load was applied by a piston of 1.4 mm diameter and 0.5 mm/min crosshead speed using the universal testing machine (Fig. 14).



Figure 13: Metallic platform with steel balls

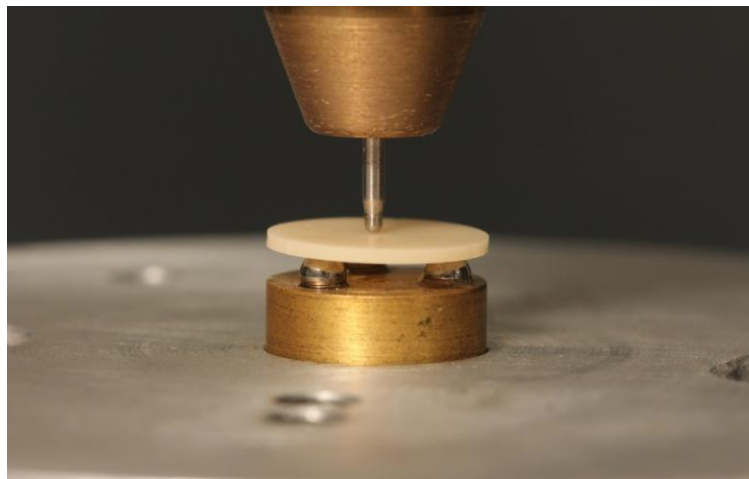


Figure 14: Close-up view of metallic platform, disc, and piston

The fracture load for each specimen was recorded (Fig. 15) and the biaxial flexural strength was calculated using the following equation:

$$S = [-0.2387P(X - Y)]/d^2$$

Where: *S*: biaxial flexural strength (MPa); *P*: fracture load (N); *d*: specimen disk thickness at fracture origin (mm).

$$X: (1 + \nu) \ln(r_2 / r_3)^2 + [(1 - \nu) / 2] (r_2 / r_3)^2$$

$$Y: (1 + \nu) [1 + \ln(r_1 / r_3)^2] + (1 - \nu) (r_1 / r_3)^2$$

ν is Poisson's ratio (0.25), r_1 is the radius of the support circle, r_2 is the radius of the loaded area, and r_3 is the radius of the specimen. The results for the specimens in MPa were later recorded.

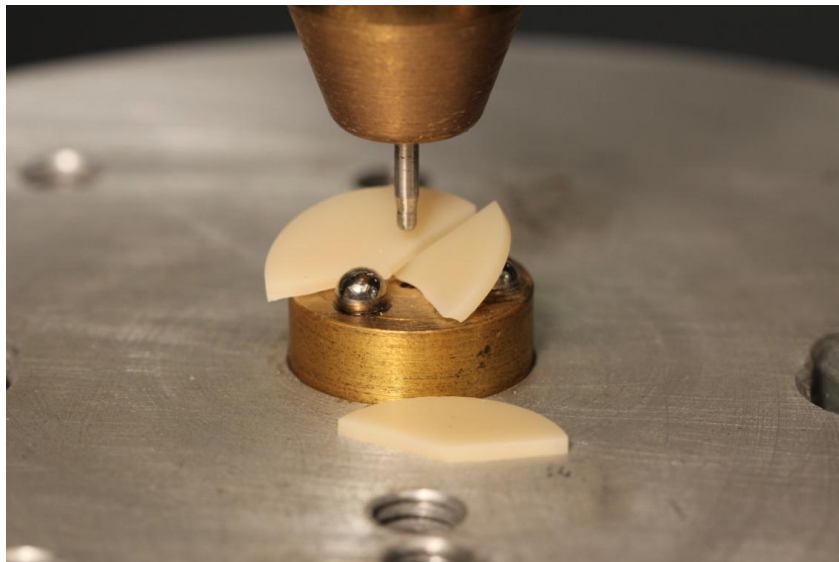


Figure 15: Fractured zirconia disc

4.6. Vickers hardness test

A piece from each specimen in each subgroup was selected for hardness measurement. Each piece was placed on the platform of a hardness testing machine (Zwick 3212, Zwick, Ulm, Germany) (Fig. 16). A load of 5 kg was applied on the specimens for a period of 10 seconds (Fig. 17). The indentation was observed under 20× magnification, and the length of its diagonal was measured in μm (Fig. 18). The Vickers hardness number (VHN) was later obtained according to the following equation: $VHN = 1.8544 \times (F/d^2)$

Where VHN is the Vickers hardness number, *F* is the applied load expressed in Kg, and *d* is the mean length of the diagonals of the indentation (mm). This procedure was done

Materials and methods

three times at three different areas for every specimen and their average was recorded.



Figure 16: Vickers hardness testing machine

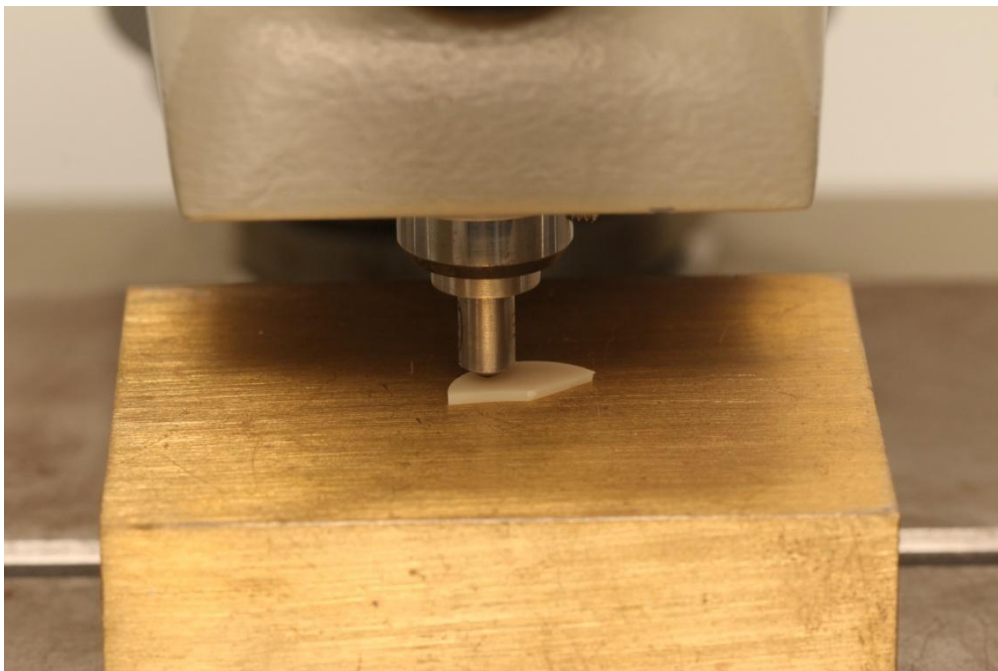


Figure 17: Vickers hardness indenter



Figure 18: Observation of indentation under 20× magnification

4.7. Data management and analysis

The collected data was revised, coded, tabulated and introduced to a PC using Statistical package for Social Science (SPSS 20.0 for windows; SPSS Inc, Chicago, IL, 2011). Data was presented and suitable analysis was done according to the type of data obtained for each parameter.

i. Descriptive statistics

- Mean
- Standard deviation (\pm SD)

ii. Analytical statistics

1. **Two-way ANOVA** was used to examine the effect of sintering temperatures and times on each of the tested variables.
2. **Tukey's HSD post-hoc test:** Once it was determined that differences existed between means, Tukey's HSD multiple comparison tests were conducted to determine which means differ.

P- value: level of significance

- a) $P > 0.05$: Non significant (NS).
- b) $P \leq 0.05$: Significant (S).
- c) $P \leq 0.01$: Highly significant

5. Results

5.1. Color reproduction

Delta E results (Means \pm SD) for all nine subgroups are summarized in Table 4 and graphically depicted in Figure 19.

Table 4: Mean and standard deviation of delta E for all subgroups

		Sintering Temp/ $^{\circ}$ C					
		1,460		1,530		1,600	
		Delta E		Delta E		Delta E	
		Mean	Standard Deviation	Mean	Standard Deviation	Mean	Standard Deviation
Sintering holding time/h	1	4.4	0.3	3.1	0.1	2.4	0.1
	2	4.0	0.1	2.8	0.3	2.2	0.1
	4	3.8	0.1	2.9	0.1	2.2	0.1

Table 5: Multiple comparisons showing the significance of changes in sintering time on delta E

(I) Sintering holding time/h	(J) Sintering holding time/h	Mean Difference (I-J)	p-value
1	2	.333 [*]	≤ 0.01
	4	.367 [*]	≤ 0.01
2	4	.033	> 0.05

Table 6: Multiple comparisons showing the significance of changes in sintering temperature on delta E

(I) Sintering Temp/ $^{\circ}$ C	(J) Sintering Temp/ $^{\circ}$ C	Mean Difference (I-J)	p-value
1,460	1,530	1.163 [*]	≤ 0.01
	1,600	1.847 [*]	≤ 0.01
1,530	1,600	.683 [*]	≤ 0.01

Results

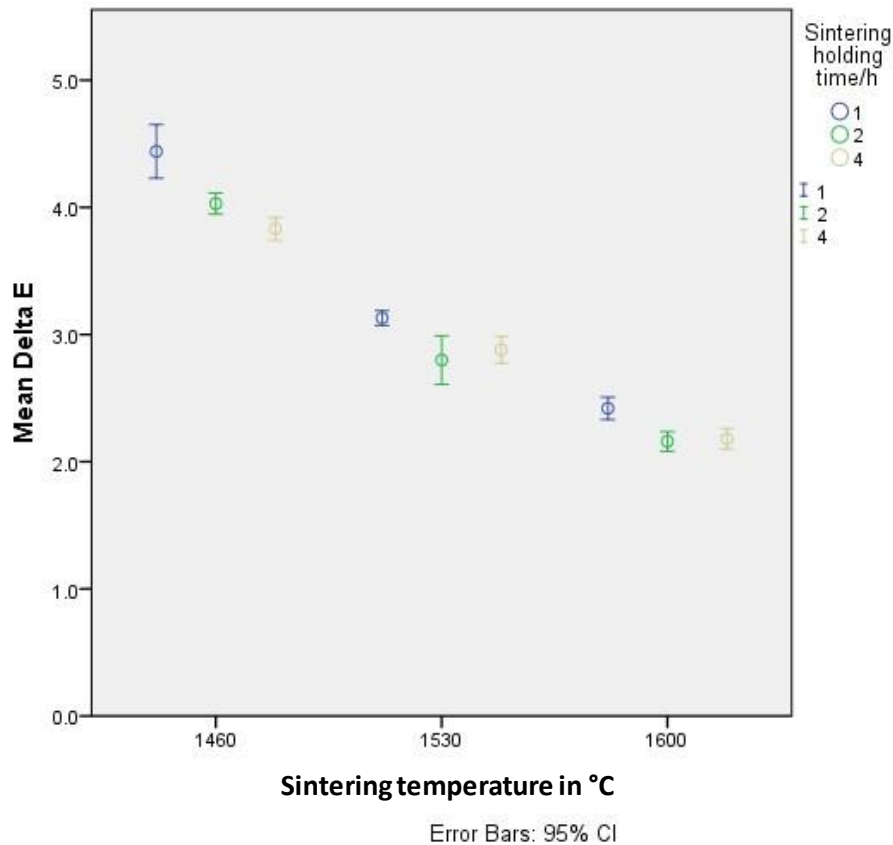


Figure 19: Graphical representation showing means and confidence intervals of delta E for all subgroups

Two-way ANOVA revealed significant differences in the ΔE between the subgroups when sintered using different sintering temperatures and times ($P \leq 0.01$). Tukey's HSD tests revealed that there was a significant decrease in the ΔE as the sintering temperature increased. It also revealed that there was no significant difference in the ΔE between the 2 and 4 hours sintering holding times however, both showed a significant decrease when compared to the 1 hour sintering holding time.

None of the subgroups showed any unacceptable color results, with the sintering temperatures 1,460°C and 1,530°C groups showing clinically acceptable results and the sintering temperature 1,600°C group showing clinically imperceptible color results.

Results

5.2. Translucency

Contrast ratio results (Means \pm SD) for all nine subgroups are summarized in Table 7 and graphically depicted in Figure 20.

Table 7: Mean and standard deviation of CR for all subgroups

		Sintering Temp/ $^{\circ}$ C					
		1460		1530		1600	
		CR		CR		CR	
		Mean	Standard Deviation	Mean	Standard Deviation	Mean	Standard Deviation
Sintering holding time/h	1	0.75	0.02	0.72	0.01	0.71	0.01
	2	0.75	0.03	0.71	0.01	0.70	0.01
	4	0.71	0.01	0.69	0.01	0.68	0.01

Table 8: Multiple comparisons showing the significance of changes of sintering time on CR

(I) Sintering holding time/h	(J) Sintering Time/h	Mean Difference (I-J)	p-value
1	2	.0030	>0.05
	4	.0300*	\leq 0.01
2	4	.0270*	\leq 0.01

Table 9: Multiple comparisons showing the significance of changes in sintering temperature on CR

(I) Sintering Temp/ $^{\circ}$ C	(J) Sintering Temp/ $^{\circ}$ C	Mean Difference (I-J)	p-value
1,460	1,530	.0310*	\leq 0.01
	1,600	.0370*	\leq 0.01
1,530	1,600	.0060	>0.05

Results

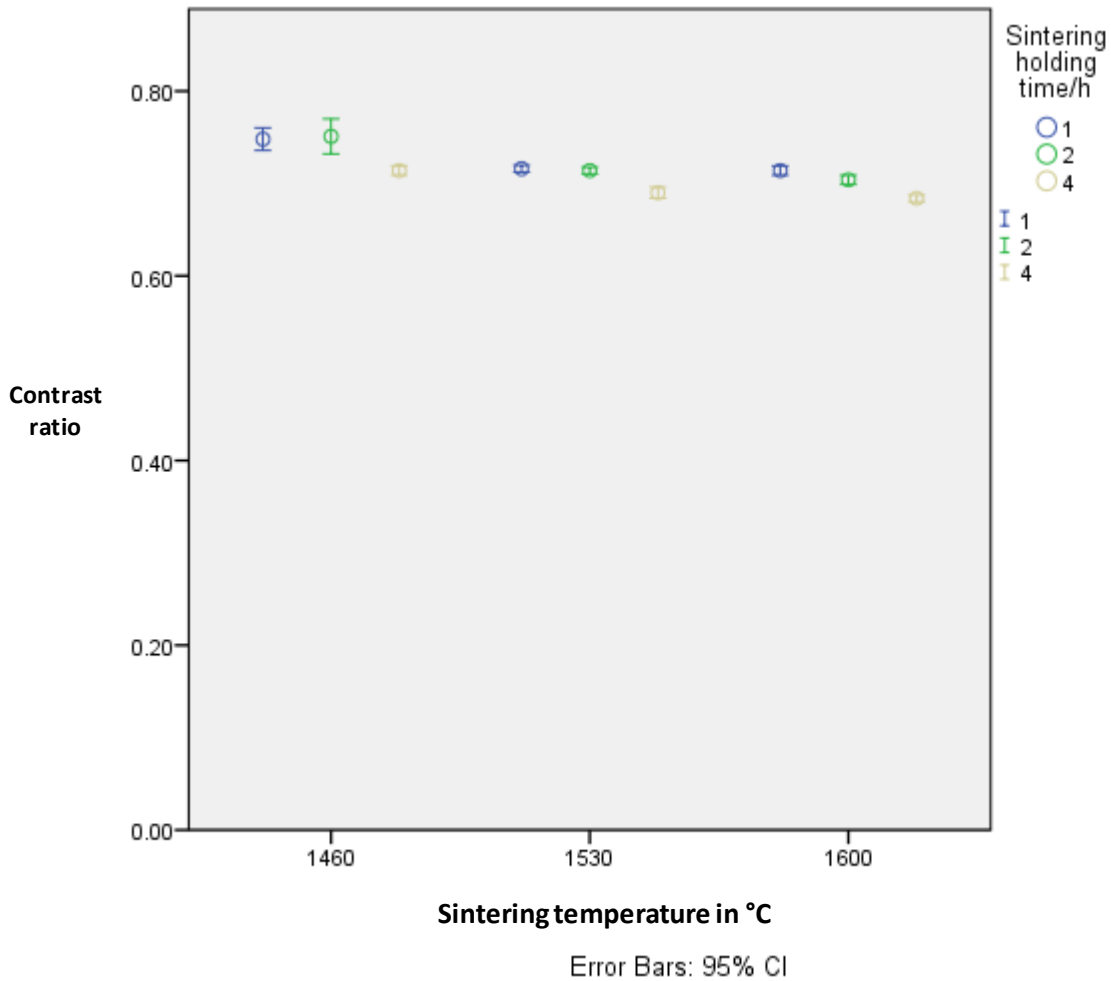


Figure 20: Graphical representation showing means and confidence intervals of CR for all subgroups

Two-way ANOVA revealed significant differences in the CR between the subgroups when sintered using different sintering temperatures and times ($P \leq 0.01$). Tukey's HSD tests revealed that there was a significant decrease in the CR when comparing the sintering temperatures 1,460°C to the 1,530°C and 1,600°C. It also revealed that there was a significant decrease in the CR when comparing the 1 and 2 hours sintering holding times to the 4 hours ($P \leq 0.01$).

5.3. Surface roughness

Surface roughness results (Means±SD) for all nine subgroups are summarized in Table 10 and graphically depicted in Figure 21.

Table 10: Mean and standard deviation of Ra for all subgroups

		Sintering Temp/°C						p-value
		1,460		1,530		1,600		
		Ra		Ra		Ra		
		Mean	Standard Deviation	Mean	Standard Deviation	Mean	Standard Deviation	
Sintering holding time/h	1	1.030	0.190	1.026	0.304	0.898	0.191	>0.05
	2	1.023	0.164	0.878	0.215	0.957	0.242	>0.05
	4	0.991	0.198	1.069	0.086	0.826	0.161	>0.05
p-value		>0.05		>0.05		>0.05		

Two-way ANOVA revealed no significant differences in the Ra between the subgroups when sintered using different sintering times and temperatures (P>0.05).

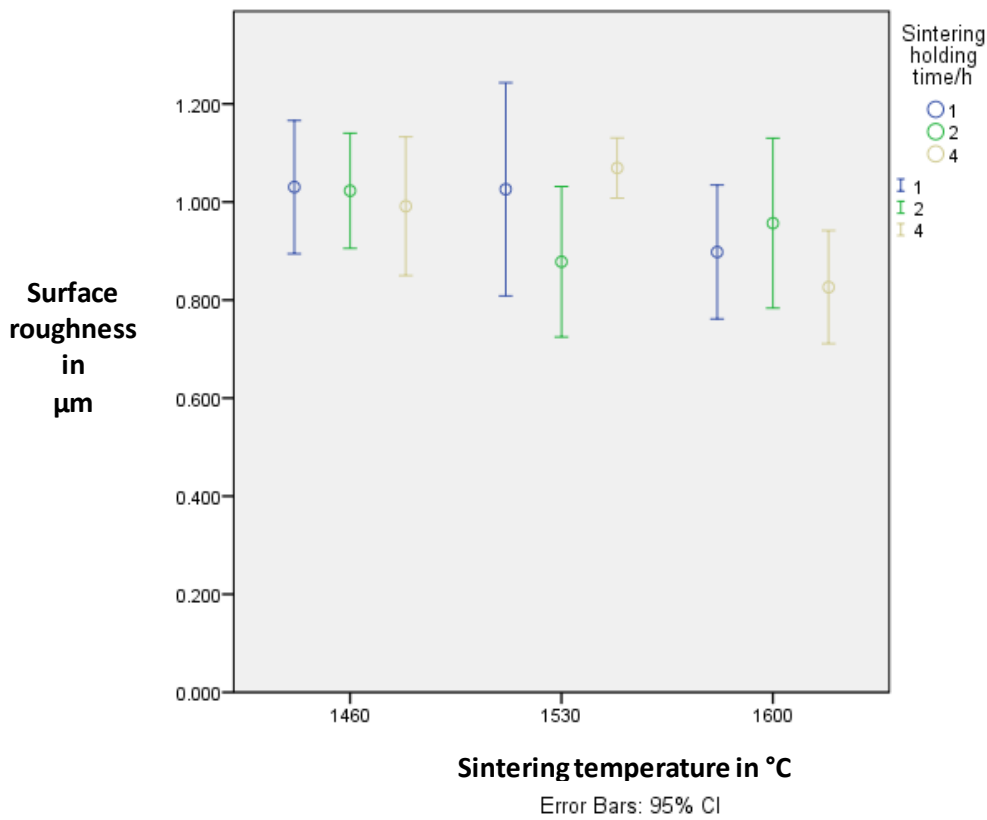


Figure 21: Graphical representation showing means and confidence intervals of Ra for all subgroups

5.4. Microstructure analysis

All specimens tested for XRD showed only a tetragonal ZrO₂ phase in the characteristic peak but no monoclinic phase. They all showed the same diffraction pattern with identical diffraction peaks (Fig. 22). However, specimens showed a significant increase in the average grain size as the sintering temperature increased ($P \leq 0.05$). Specimens sintered at 2 and 4 hours sintering holding time also showed a statistically significant increase in the average grain size ($P \leq 0.05$) when compared to specimens sintered at a 1 hour sintering holding time (Table 11).

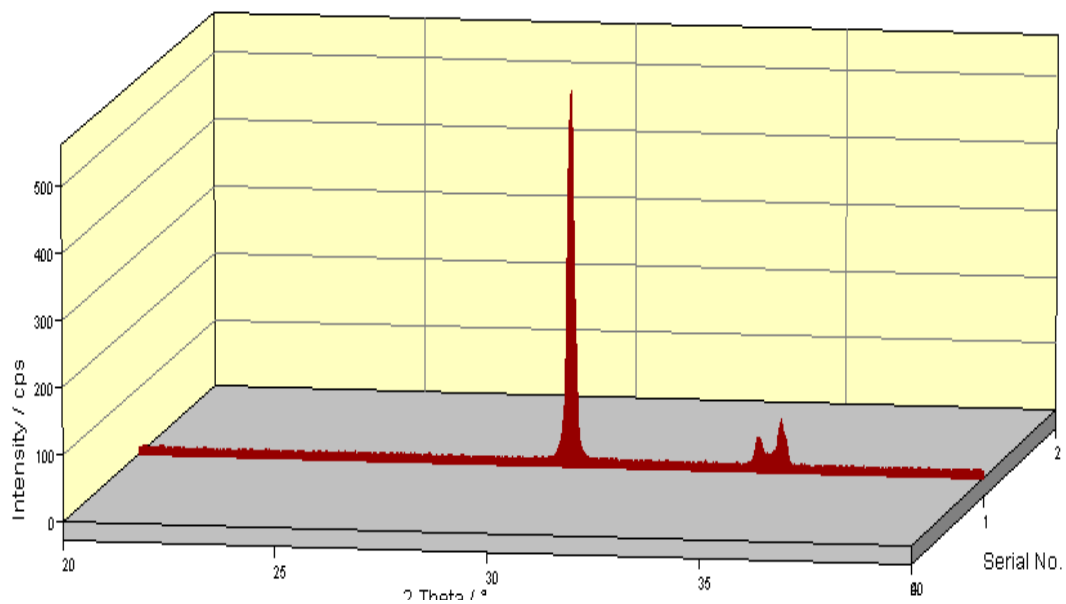


Figure 22: Graph showing tetragonal phase characteristic peaks

Table 11: Mean and standard deviation of grain size in μm for all subgroups

		Sintering Temp/°C						p-value
		1,460		1,530		1,600		
		Grain size in μm		Grain size in μm		Grain size in μm		
		Mean	Standard Deviation	Mean	Standard Deviation	Mean	Standard Deviation	
Sintering holding time/h	1	0.55	0.10	0.65	0.13	0.89	0.19	<0.05
	2	0.64	0.11	0.77	0.13	1.0	0.11	<0.05
	4	0.79	0.15	0.92	0.25	0.92	0.14	<0.05
p-value		<0.05		<0.05		<0.05		

5.5. Biaxial flexural strength

Biaxial flexural strength results (Means±SD) for all nine subgroups are summarized in Table 12 and graphically depicted in Figure 23.

Table 12: Mean and standard deviation of BFS for all subgroups

		Sintering Temp/°C						p-value
		1,460		1,530		1,600		
		BFS/MPa		BFS/MPa		BFS/MPa		
		Mean	Standard Deviation	Mean	Standard Deviation	Mean	Standard Deviation	
Sintering holding time/h	1	1000	96	906	70	968	142	>0.05
	2	988	107	961	87	930	79	>0.05
	4	943	140	937	137	960	58	>0.05
p-value		>0.05		>0.05		>0.05		

Two-way ANOVA revealed no significant differences in the BFS between the subgroups when sintered using different sintering times and temperatures (P>0.05).

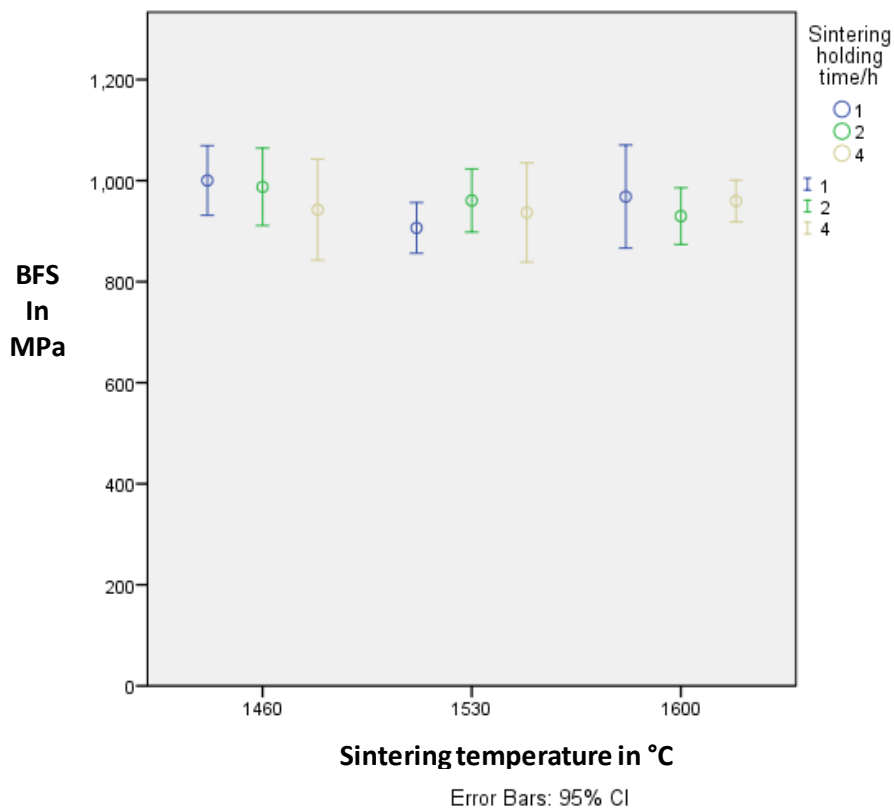


Figure 23: Graphical representation showing means and confidence intervals of BFS for all subgroups

5.6. Surface hardness

Vickers hardness number results (Means±SD) for all nine subgroups are summarized in Table 13 and graphically depicted in Figure 24.

Table 13: Mean and standard deviation of VHN for all subgroups

		Sintering Temp/°C						p-value
		1,460		1,530		1,600		
		Vickers Hardness Number		Vickers Hardness Number		Vickers Hardness Number		
		Mean	Standard Deviation	Mean	Standard Deviation	Mean	Standard Deviation	
Sintering holding time/h	1	1456	212	1553	111	1461	108	>0.05
	2	1506	123	1548	77	1507	71	>0.05
	4	1497	138	1437	74	1415	60	>0.05
p-value		>0.05		>0.05		>0.05		

Two-way ANOVA revealed no significant differences in the VHN between the subgroups when sintered using different sintering times and temperatures (P>0.05).

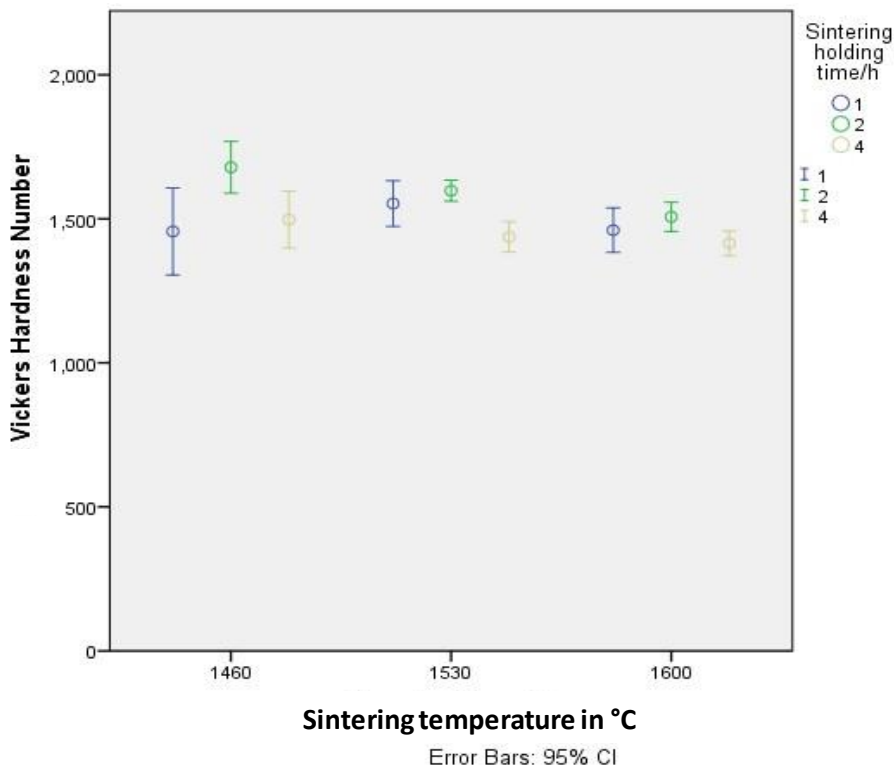


Figure 24: Graphical representation showing means and confidence intervals of VHN for all subgroups

6. Discussion

6.1. Discussion of methodology

The use of the Vita Easyshade spectrophotometer for obtaining the CIELAB coordinates is commonly used in the field of dental research.^[22, 33] In this study it was used for obtaining the ΔE and CR for the specimens.

The literature differences on tooth color acceptability and perceptibility using ΔE values is probably due to the diversity of observers, objectives and methodologies among the studies.^[6, 10, 67] Clinically the tooth or restoration context and surroundings (e.g. skin, lips, gingiva, adjacent teeth, position in the arch, shape, color, translucency, texture, salivary moisture) and the blending effect, tend to expand the clinically acceptable limit previously reported. The mean ΔE values used in this study as “clinically imperceptible” ($\Delta E < 3$), “clinically acceptable” (ΔE between 3 and 5) and “clinically unacceptable” ($\Delta E > 5$) seem to be consistent with the clinical practice considering a non-color expert, which usually is the patient’s condition.^[3, 22, 43]

The translucency of dental ceramics can be studied in three ways: through direct transmission, which can be assessed by measuring the light that reaches a detector; total transmission, which can be assessed by measuring both the light that reaches the detector and that which passes the ceramic and is scattered; and indirect measurements via spectral reflectance.^[13] In this study, we measured translucency by assessing the spectral reflectance and calculating the contrast ratio which was used by several authors for obtaining a quantitative measure of translucency for zirconia.^[19, 31, 74]

The description of surface roughness by R_a is widely established in dentistry, especially using tactile profilometry.^[27, 37] Values of R_a vary with the techniques used which makes direct comparisons difficult. The most common measurement method is using a mechanical profilometer, although widely available and relatively cheap, it is limited by the spatial dimension of the stylus, measuring force, sampling rate and by the calibration in the z -axis. Al-Nawas et al. questioned the use of this technique for the study of microtopography.^[2] Wennerberg et al. in a study comparing stylus and laser scanning techniques concluded that in general the stylus technique presented a smoother surface than laser scanning, i.e. the former underestimates surface roughness and the latter overestimates surface roughness. This was attributed to the stylus not reaching the bottom of narrow valleys and deforming surface asperities, resulting in a loss of information. In

the current study the laser scanning technique was used.^[87]

The use of XRD to determine the phases of ZrO₂ is of special importance in the dental research area. Quantitative assessment of the volume fraction of the monoclinic phase can be calculated using the equations described by Garvie et al. in 1984.^[25,81] Intensity ratio of the reflections of two phases has always been used for the quantitative analysis by X-ray diffraction. In this study it was important to identify whether the changes in the sintering parameters will cause transformation of the tetragonal crystal or not. There was no need to calculate the volume fraction of the monoclinic crystals as none of the specimens analyzed showed any monoclinic peaks but rather pure tetragonal peaks.

For brittle materials, the biaxial flexure test, 3-point flexure test, 4-point flexure test and diametral tensile test have been used.^[9] However, all methods have their limitations as none of the test specimens and test methods employed replicates the complex intra-oral stresses acting on artificial crowns.^[36,55,59] The current study used the biaxial flexural strength test. Designs for the test include ring-on-ring, piston-on-ring, ball-on-ring, ring-on-ball, ring-on-spring and piston-on-three-ball. The last method was adopted, which has the following advantages; point contact between the three stainless steel balls and the specimen disk prevents any undesirable stresses when the specimen is not flat, and the 10 mm diameter formed by the three stainless steel balls is smaller than the specimen disk diameter of 15 mm, therefore preventing edge fracture from direct loading, and simulating pure bending.^[9, 84]

6.2. Discussion of results

In the present study the effect of different sintering times and temperatures on the color reproduction, translucency, surface roughness, microstructure, biaxial flexural strength, and Vickers hardness of monolithic translucent zirconia were evaluated. Results revealed that there was a significant reduction in the ΔE and CR with the increase in either the sintering time or temperature. Mean ΔE values ranged from 4.4 till 2.2 while mean CR values ranged from 0.75 till 0.68.

Results of this study are similar to a study performed by Jiang et al. where sintering temperatures 1,350, 1,400, 1,450, and 1,500°C were used and their effect on the translucency of zirconia discs was measured. They concluded that as the sintering temperature increased also the translucency of the discs increased.^[42]

Results are also in agreement with Stawarczyk et al. as they reported a decrease in the CR of commercial zirconia core material specimens (Ceramill ZI, Amann Girrback)

Discussion

having 0.5 mm thickness from 0.85 to 0.70 as the sintering temperature increased from 1,300 to 1,700°C. Also comparing the CR of the Ceramill specimens they used to the Bruxzir specimens in the current study shows that the CR of Bruxzir zirconia is much less although the specimens had a thickness of 1 mm.^[75]

The sintering process determines the properties of ceramics by effect on the microstructure and the crystalline phases.^[21] Sintering can eliminate the interparticle pores in a granular material by atomic diffusion driven by capillary forces. As the temperature rises, the particles are sintered together and pores on grain boundaries are reduced by solid-state diffusion, so the sintered density increases.^[16] This reduction in the pores may be the main factor responsible for the reduction of the ΔE and the CR. This assumption was consistent with our results as increasing the sintering temperature and time led to an increase in the average grain size of zirconia. This also supports the fact that reducing the grain size to a nano scale as in Bruxzir zirconia will lead to fewer pores thus giving it an improved translucency compared to regular zirconia core materials. Also the increase in the sintered density of the zirconia may lead to a more uniform crystalline arrangement thus promoting better specular reflection, light transmission and penetration, and less refraction.

Results of this study also showed that there was no effect of the changes done in the sintering parameters on the surface roughness of the specimens. Since there was no significant differences between the subgroups regarding the surface roughness, it can be also assumed that the reduction in the pores between the grains is not enough to produce a significant difference. It can also be assumed that the changes in the contrast ratio and ΔE are mainly due to changes in the microstructure rather than changes in surface morphology.

Concerning the biaxial flexural strength, raising the sintering holding time from 1 to 4 hours and the sintering temperature from 1,460°C to 1,600°C did not have any significant effect on the results in this study. It needs to be noticed that the study was performed by static loading test and that the dynamic (fatigue) test would imitate closer clinical masticatory forces. However, Itinoche et al. found no significant differences between the dynamic and static loading tests on the biaxial flexural strength of zirconia specimens.^[40]

Biaxial flexural strength results are in agreement with the results of the study by Hjerpe et al. They rose the sintering time from 2 hours 40 mins to 5 hours and there was no significant effect on the biaxial flexural strength of the commercial core zirconia

Discussion

specimens (ICE Zirkon, ZirkonZahn, Italy).^[35]

Stawarczyk et al. in 2013 also found no significant difference in the biaxial flexural strength of commercial core zirconia specimens (Ceramill ZI, Amann Girrbach) when raising the sintering temperature from 1,400°C to 1,550°C. However, the biaxial flexural strength decreased significantly below 1,400°C and above 1,550°C.^[75]

In a similar study by Jiang et al. they concluded that raising the sintering temperature above 1550°C will lead to migration of the yttrium to the grain boundaries thus lowering the biaxial flexural strength of the zirconia.^[42] However, this was not in agreement with the results of this study as even when the sintering temperature was raised to 1,600°C the biaxial flexural strength was not affected nor the average grain size increased beyond 1 µm. It has to be mentioned that all of our specimens were sintered as milled and they were not polished, thus comparing our biaxial flexural strength values to values from other studies with polished specimens is questionable as in several studies polished specimens showed higher BFS than as-sintered specimens.^[39, 61]

Kosmac et al. found that after aging in 4% acetic acid solution the relative amount of monoclinic zirconia exceeded 14.7–30% depending on how fine-grained the material was. The more fine-grained material was, less monoclinic zirconia was found.^[46] Also Sato and Shimada found that the rate of tetragonal to monoclinic transformation slightly increased with increasing grain-size in the sintered zirconia.^[71] Swain has shown that the grain-size of zirconia is increasing after longer sintering time.^[77] This was also seen in the current study as the grain-size was smaller in the groups with shorter sintering time

In the current study, there was no difference between the groups regarding Vickers surface hardness. This coincides with not detecting any monoclinic phase in the specimens since theoretically monoclinic phase transition at surface would cause compressive stress to the outer layer of zirconia, which could increase surface hardness and the biaxial flexural strength.

A limitation of this study was that the intraoral environment, with respect to variables such as temperature and humidity, was not simulated. The effect of different sintering parameters on zirconia specimens after several aging procedures should still be investigated.

7. Conclusions

Within the limitations of this study, the following conclusions could be drawn:

1. There is a significant decrease in the ΔE thus better color reproduction of pre-shaded monolithic translucent zirconia as the sintering time and temperature increased.
2. Increasing the time and temperature of zirconia sintering lead to enhanced translucency.
3. Increasing sintering time and temperature of zirconia will lead to an increase in grain size.
4. Sintering zirconia within the range of parameters selected did not significantly affect surface roughness, biaxial flexural strength, and surface hardness nor did it cause any monoclinic phase transformation

8. Summary

This study was designed to evaluate the effect of different sintering times and temperatures on the color reproduction, translucency, surface roughness, biaxial flexural strength and surface hardness of monolithic translucent zirconia.

Ninety disc shaped specimens having 15 mm diameter and 1 mm thickness were milled using a milling machine (Datron D5, Datron AG, Muhltal-Traisa, Germany) from translucent zirconia blanks (Bruzir, Glidewell, Frankfurt, Germany) with the shade A3. Specimens were divided into three groups (n=30) according to the sintering temperature (1460°C, 1530°C, 1600°C) and each group was later subdivided into three subgroups (n=10) according to the sintering holding time (1, 2, 4 hours).

Delta E was obtained for the specimens after measuring the CIELAB coordinates for each disc using a spectrophotometer (Vita Easysshade, Vita, Bad Säckingen, Germany) and comparing the outcome to the standard coordinates of the shade A3. The contrast ratio (CR) was calculated for each specimen to assess translucency after obtaining the CIELAB coordinates when backed with a white and black background. This ratio tends toward unity for opaque materials and toward zero for transparent materials. A 3D laser microscope (Keyence VX-100, Keyence, Neu-Isenburg, Germany) was used to scan the discs surface and measure the surface roughness.

Three samples from each subgroup were analyzed using an X-ray diffractometer (Seifert PTS-3000, General Electric, Connecticut, USA) to detect the ZrO₂ tetragonal and monoclinic phases present. Samples were subject to Cu K alpha radiation with a range of 20°-40°, step size of 0.02° and the scan time per step was 10 seconds. The biaxial flexural strength test was performed using piston-on-three balls technique according to the ISO 6872 specifications. A universal testing machine (Zwick Z010, Zwick, Ulm, Germany) at a crosshead speed of 0.5 mm/min was used to conduct the test and the fracture load was used to calculate the biaxial flexural strength in MPa. Vickers surface hardness test was performed using a hardness testing machine (Zwick 3212, Zwick, Ulm, Germany) on the broken samples. A load of 5 kg was applied using the indenter on the specimens for a period of 10 seconds and the indentation was observed under a magnification of 20×. Results were tabulated and statistically analyzed using two-way ANOVA and Tukeys HSD post hoc test.

Statistical analysis revealed a significant decrease in the ΔE and the CR as the sintering time and temperature increased. No significant changes were observed among

Summary

the groups regarding the surface roughness, biaxial flexural strength and surface hardness. Regarding the XRD analysis, all of the tested samples showed only tetragonal phase characteristic peaks.

With the limitations of this study, it can be concluded that increasing the sintering time and temperature within the range selected will lead to better color reproduction, enhanced translucency, and larger grain size. However, the change in sintering parameters within the range selected will have no effect on surface roughness, biaxial flexural strength and Vickers hardness.

Zusammenfassung

Ziel dieser Studie war es, den Einfluss von verschiedenen Sinterzeiten und Temperaturen auf die Farbwiedergabe, Transparenz, Oberflächenrauigkeit, biaxiale Biegefestigkeit und Oberflächenhärte von monolithischem transluzentem Zirkonoxid zu evaluieren.

Neunzig scheibenförmige Proben mit 15 mm Durchmesser und 1 mm Dicke wurden aus Zirkonoxidrohlingen der Firma Bruxzir (Glidewell, Frankfurt, Deutschland) mit der Farbe A3 gefräst. Die Proben wurden randomisiert in drei Gruppen ($n = 30$) nach der Sintertemperatur (1460°C, 1530°C, 1600°C) aufgeteilt und jede Gruppe wurde später ebenfalls randomisiert in drei Untergruppen ($n = 10$) nach der Sinterhaltezeit unterteilt (1, 2 und 4 Stunden) aufgeteilt.

Die Veränderung der Farbe ΔE wurde für die Proben durch Messung der CIELAB-Koordinaten für jede Scheibe mit einem Spektralphotometer (Vita Easysshade, Bad Säckingen, Deutschland) und dem Vergleich der Ergebnisse zu den Standard-Koordinaten der Farbe A3 ermittelt.

Das Kontrastverhältnis (CR) wurde für jede Probe berechnet, um die Transparenz nach dem Erhalt der CIELAB-Koordinaten, als sie auf einem weißen und schwarzen Hintergrund vermessen wurden zu bewerten. Für opake Materialien ergibt sich ein Kontrastverhältnis von $CR \approx 1$, transparente Materialien weisen ein Kontrastverhältnis von $CR \approx 0$ auf.

Ein Lasermikroskop Keyence VX-100 3D wurde verwendet, um die Oberfläche der Proben zu scannen und die Oberflächenrauheit zu messen.

Drei Proben jeder Untergruppe wurden mit Hilfe der Röntgenbeugung (XRD) untersucht, um den Anteil der tetragonalen und monoklinen Phasen an der Zirkonoxidoberfläche zu bestimmen. Die Proben wurden mit einer Cu-K α -Strahlung unter einem Winkelbereich von 20°-40° in Schritten von 0,04° bestrahlt. Dabei betrug die Scanzeit pro Schritt 10 s.

Zur Bestimmung der biaxialen Biegefestigkeit wurden die Proben auf drei Kugeln gelagert und dann mit einem Stempel gemäß der ISO 6872-Spezifikationen belastet. Für den Test wurde eine Universalprüfmaschine (Z010, Zwick, Ulm, Deutschland) verwendet. Die biaxiale Biegefestigkeit in MPa wurde dann über eine Formel mit Hilfe der Kraft ermittelt, bei der es zum Bruch der Probe kam.

Der Härte test nach Vickers wurde mit der Härteprüfmaschine (Zwick 3212, Zwick,

Summary

Ulm, Deutschland) auf den frakturierten Proben durchgeführt. Der Eindringkörper wurde mit einer Last von ca. 49 N (5 kg) auf die Proben für eine Dauer von 10 s auf die Proben gedrückt. Der dabei entstandene Abdruck wurde bei einer zwanzigfachen Vergrößerung vermessen.

Die Ergebnisse wurden tabellarisch erfasst und mit einer zweifaktoriellen Varianzanalyse und einem anschließenden post-hoc Tukeys HSD-Test statistisch ausgewertet. Die statistische Analyse ergab eine signifikante Abnahme von ΔE und CR, wenn die Sinterzeit und die Temperatur erhöht wurden. In der Oberflächenrauheit, biaxialen Biegefestigkeit und der Oberflächenhärte wurden keine signifikanten Veränderungen zwischen den Gruppen beobachtet. In Bezug auf die Röntgenbeugungsanalyse, zeigten alle getesteten Proben nur die charakteristischen Peaks für die tetragonale Phase.

9. References

1. 6872, Dentistry-ceramic materials. International Organization for Standardization, 2006; Geneva.
2. Al-Nawas, B., Grotz, K.A., Gotz, H., Heinrich, G., Rippin, T.G., Stender, T.E., Duschner, H., and Wagner, W., Validation of three-dimensional surface characterising methods: Scanning electron microscopy and confocal laser scanning microscopy. *Scanning*, 2001; 23: 227-31.
3. Alghazali, N., Burnside, G., Moallem, M., Smith, P., Preston, A., and Jarad, F.D., Assessment of perceptibility and acceptability of color difference of denture teeth. *J Dent*, 2012; 40 Suppl 1: e10-7.
4. Anusavice, K.J., Recent developments in restorative dental ceramics. *J Am Dent Assoc*, 1993; 124: 72-4, 76-8, 80-4.
5. Attia, A., Bond strength of three luting agents to zirconia ceramic - influence of surface treatment and thermocycling. *J Appl Oral Sci*, 2011; 19: 388-95.
6. Azer, S.S., Ayash, G.M., Johnston, W.M., Khalil, M.F., and Rosenstiel, S.F., Effect of esthetic core shades on the final color of ips empress all-ceramic crowns. *J Prosthet Dent*, 2006; 96: 397-401.
7. Bachhav, V.C. and Aras, M.A., Zirconia-based fixed partial dentures: A clinical review. *Quintessence Int*, 2011; 42: 173-82.
8. Baldissara, P., Llukacej, A., Ciocca, L., Valandro, F.L., and Scotti, R., Translucency of zirconia copings made with different cad/cam systems. *J Prosthet Dent*, 2010; 104: 6-12.
9. Ban, S. and Anusavice, K.J., Influence of test method on failure stress of brittle dental materials. *J Dent Res*, 1990; 69: 1791-9.
10. Barath, V.S., Faber, F.J., Westland, S., and Niedermeier, W., Spectrophotometric analysis of all-ceramic materials and their interaction with luting agents and different backgrounds. *Adv Dent Res*, 2003; 17: 55-60.
11. Beuer, F., Stimmelmayer, M., Gueth, J.F., Edelhoff, D., and Naumann, M., In vitro performance of full-contour zirconia single crowns. *Dent Mater*, 2012; 28: 449-56.
12. Bona, A.D., Anusavice, K.J., and DeHoff, P.H., Weibull analysis and flexural strength of hot-pressed core and veneered ceramic structures. *Dent Mater*, 2003; 19: 662-9.
13. Brodbelt, R.H., O'Brien, W.J., and Fan, P.L., Translucency of dental porcelains. *J Dent*

References

- Res, 1980; 59: 70-5.
14. Casucci, A., Mazzitelli, C., Monticelli, F., Toledano, M., Osorio, R., Osorio, E., Papacchini, F., and Ferrari, M., Morphological analysis of three zirconium oxide ceramics: Effect of surface treatments. *Dent Mater*, 2010; 26: 751-60.
 15. Chai, J., Chu, F.C., Chow, T.W., and Liang, B.M., Chemical solubility and flexural strength of zirconia-based ceramics. *Int J Prosthodont*, 2007; 20: 587-95.
 16. Chen, I.W. and Wang, X.H., Sintering dense nanocrystalline ceramics without final-stage grain growth. *Nature*, 2000; 404: 168-71.
 17. Chintapalli, R.K., Marro, F.G., Jimenez-Pique, E., and Anglada, M., Phase transformation and subsurface damage in 3y-tzp after sandblasting. *Dent Mater*, 2013; 29: 566-72.
 18. Christel, P., Meunier, A., Dorlot, J.M., Crolet, J.M., Witvoet, J., Sedel, L., and Boutin, P., Biomechanical compatibility and design of ceramic implants for orthopedic surgery. *Ann N Y Acad Sci*, 1988; 523: 234-56.
 19. Chu, F.C., Chow, T.W., and Chai, J., Contrast ratios and masking ability of three types of ceramic veneers. *J Prosthet Dent*, 2007; 98: 359-64.
 20. Demir, N., Subasi, M.G., and Ozturk, A.N., Surface roughness and morphologic changes of zirconia following different surface treatments. *Photomed Laser Surg*, 2012; 30: 339-45.
 21. Denry, I. and Kelly, J.R., State of the art of zirconia for dental applications. *Dent Mater*, 2008; 24: 299-307.
 22. Douglas, R.D., Steinhauer, T.J., and Wee, A.G., Intraoral determination of the tolerance of dentists for perceptibility and acceptability of shade mismatch. *J Prosthet Dent*, 2007; 97: 200-8.
 23. Elmaria, A., Goldstein, G., Vijayaraghavan, T., Legeros, R.Z., and Hittelman, E.L., An evaluation of wear when enamel is opposed by various ceramic materials and gold. *J Prosthet Dent*, 2006; 96: 345-53.
 24. Flinn, B.D., deGroot, D.A., Mancl, L.A., and Raigrodski, A.J., Accelerated aging characteristics of three yttria-stabilized tetragonal zirconia polycrystalline dental materials. *J Prosthet Dent*, 2012; 108: 223-30.
 25. Garvie, R. and Nicholson, P., Phase analysis in zirconia systems. *J Am Ceram Soc*, 1972; 55: 303-5.
 26. Ghazal, M. and Kern, M., The influence of antagonistic surface roughness on the wear of human enamel and nanofilled composite resin artificial teeth. *J Prosthet Dent*, 2009;

References

- 101: 342-9.
27. Glavina, D., Skrinjaric, I., Mahovic, S., and Majstorovic, M., Surface quality of cerecad/cam ceramic veneers treated with four different polishing systems. *Eur J Paediatr Dent*, 2004; 5: 30-4.
 28. Guazzato, M., Albakry, M., Ringer, S.P., and Swain, M.V., Strength, fracture toughness and microstructure of a selection of all-ceramic materials. Part ii. Zirconia-based dental ceramics. *Dent Mater*, 2004; 20: 449-56.
 29. Guazzato, M., Albakry, M., Swain, M.V., and Ironside, J., Mechanical properties of in-ceram alumina and in-ceram zirconia. *Int J Prosthodont*, 2002; 15: 339-46.
 30. Guazzato, M., Quach, L., Albakry, M., and Swain, M.V., Influence of surface and heat treatments on the flexural strength of y-tzp dental ceramic. *J Dent*, 2005; 33: 9-18.
 31. Heffernan, M.J., Aquilino, S.A., Diaz-Arnold, A.M., Haselton, D.R., Stanford, C.M., and Vargas, M.A., Relative translucency of six all-ceramic systems. Part i: Core materials. *J Prosthet Dent*, 2002; 88: 4-9.
 32. Helmer, J. and Driskell, T., Reserach on bioceramics. Symposium on use of ceramics as surgical implants. South Carolina (USA), 1969; Clemson University.
 33. Heydecke, G., Zhang, F., and Razzoog, M.E., In vitro color stability of double-layer veneers after accelerated aging. *J Prosthet Dent*, 2001; 85: 551-7.
 34. Hjerppe, J., Narhi, T., Froberg, K., Vallittu, P.K., and Lassila, L.V., Effect of shading the zirconia framework on biaxial strength and surface microhardness. *Acta Odontol Scand*, 2008; 66: 262-7.
 35. Hjerppe, J., Vallittu, P.K., Froberg, K., and Lassila, L.V., Effect of sintering time on biaxial strength of zirconium dioxide. *Dent Mater*, 2009; 25: 166-71.
 36. Huang, C.W. and Hsueh, C.H., Piston-on-three-ball versus piston-on-ring in evaluating the biaxial strength of dental ceramics. *Dent Mater*, 2011; 27: e117-23.
 37. Hultstrom, A.K. and Bergman, M., Polishing systems for dental ceramics. *Acta Odontol Scand*, 1993; 51: 229-34.
 38. Ilie, N. and Stawarczyk, B., Quantification of the amount of blue light passing through monolithic zirconia with respect to thickness and polymerization conditions. *J Prosthet Dent*, 2015; 113: 114-21.
 39. Iseri, U., Ozkurt, Z., Yalniz, A., and Kazazoglu, E., Comparison of different grinding procedures on the flexural strength of zirconia. *J Prosthet Dent*, 2012; 107: 309-15.
 40. Itinoche, K.M., Özcan, M., Bottino, M.A., and Oyafuso, D., Effect of mechanical cycling on the flexural strength of densely sintered ceramics. *Dent Mater*, 2006; 22:

References

- 1029-34.
41. Janyavula, S., Lawson, N., Cakir, D., Beck, P., Ramp, L.C., and Burgess, J.O., The wear of polished and glazed zirconia against enamel. *J Prosthet Dent*, 2013; 109: 22-9.
 42. Jiang, L., Liao, Y., Wan, Q., and Li, W., Effects of sintering temperature and particle size on the translucency of zirconium dioxide dental ceramic. *J Mater Sci Mater Med*, 2011; 22: 2429-35.
 43. Johnston, W.M. and Kao, E.C., Assessment of appearance match by visual observation and clinical colorimetry. *J Dent Res*, 1989; 68: 819-22.
 44. Kim, M.J., Ahn, J.S., Kim, J.H., Kim, H.Y., and Kim, W.C., Effects of the sintering conditions of dental zirconia ceramics on the grain size and translucency. *J Adv Prosthodont*, 2013; 5: 161-6.
 45. Kohorst, P., Brinkmann, H., Li, J., Borchers, L., and Stiesch, M., Marginal accuracy of four-unit zirconia fixed dental prostheses fabricated using different computer-aided design/computer-aided manufacturing systems. *Eur J Oral Sci*, 2009; 117: 319-25.
 46. Kosmac, T., Oblak, C., Jevnikar, P., Funduk, N., and Marion, L., Strength and reliability of surface treated y-tzp dental ceramics. *J Biomed Mater Res*, 2000; 53: 304-13.
 47. Li, Q., Yu, H., and Wang, Y.N., Spectrophotometric evaluation of the optical influence of core build-up composites on all-ceramic materials. *Dent Mater*, 2009; 25: 158-65.
 48. Long, H.A., *Moving to monolithic*. Inside dent, 2011.
 49. Luthardt, R.G., Holzner, M.S., Rudolph, H., Herold, V., and Walter, M.H., Cad/cam-machining effects on y-tzp zirconia. *Dent Mater*, 2004; 20: 655-62.
 50. Manicone, P.F., Rossi Iommetti, P., and Raffaelli, L., An overview of zirconia ceramics: Basic properties and clinical applications. *J Dent*, 2007; 35: 819-26.
 51. Marinis, A., Aquilino, S.A., Lund, P.S., Gratton, D.G., Stanford, C.M., Diaz-Arnold, A.M., and Qian, F., Fracture toughness of yttria-stabilized zirconia sintered in conventional and microwave ovens. *J Prosthet Dent*, 2013; 109: 165-71.
 52. Marquardt, P. and Strub, J.R., Survival rates of ips empress 2 all-ceramic crowns and fixed partial dentures: Results of a 5-year prospective clinical study. *Quintessence Int*, 2006; 37: 253-9.
 53. Miyagawa, Y., Powers, J.M., and O'Brien, W.J., Optical properties of direct restorative materials. *J Dent Res*, 1981; 60: 890-4.
 54. Molin, M.K. and Karlsson, S.L., Five-year clinical prospective evaluation of zirconia-based denzir 3-unit fpls. *Int J Prosthodont*, 2008; 21: 223-7.

References

55. Neiva, G., Yaman, P., Dennison, J.B., Razzoog, M.E., and Lang, B.R., Resistance to fracture of three all-ceramic systems. *J Esthet Dent*, 1998; 10: 60-6.
56. Olivera, A.B., Matson, E., and Marques, M.M., The effect of glazed and polished ceramics on human enamel wear. *Int J Prosthodont*, 2006; 19: 547-8.
57. Özcan, M., Melo, R.M., Souza, R.O., Machado, J.P., Felipe Valandro, L., and Bottino, M.A., Effect of air-particle abrasion protocols on the biaxial flexural strength, surface characteristics and phase transformation of zirconia after cyclic loading. *J Mech Behav Biomed Mater*, 2013; 20: 19-28.
58. Ozturk, O., Uludag, B., Usumez, A., Sahin, V., and Celik, G., The effect of ceramic thickness and number of firings on the color of two all-ceramic systems. *J Prosthet Dent*, 2008; 100: 99-106.
59. Pallis, K., Griggs, J.A., Woody, R.D., Guillen, G.E., and Miller, A.W., Fracture resistance of three all-ceramic restorative systems for posterior applications. *J Prosthet Dent*, 2004; 91: 561-9.
60. Papanagiotou, H.P., Morgano, S.M., Giordano, R.A., and Pober, R., In vitro evaluation of low-temperature aging effects and finishing procedures on the flexural strength and structural stability of y-tzp dental ceramics. *J Prosthet Dent*, 2006; 96: 154-64.
61. Pereira, G.K., Amaral, M., Simoneti, R., Rocha, G.C., Cesar, P.F., and Valandro, L.F., Effect of grinding with diamond-disc and -bur on the mechanical behavior of a y-tzp ceramic. *J Mech Behav Biomed Mater*, 2014; 37: 133-40.
62. Piconi, C. and Maccauro, G., Zirconia as a ceramic biomaterial. *Biomaterials*, 1999; 20: 1-25.
63. Raigrodski, A.J., Hillstead, M.B., Meng, G.K., and Chung, K.H., Survival and complications of zirconia-based fixed dental prostheses: A systematic review. *J Prosthet Dent*, 2012; 107: 170-7.
64. Rinke, S. and Fischer, C., Range of indications for translucent zirconia modifications: Clinical and technical aspects. *Quintessence Int*, 2013; 44: 557-66.
65. Rinke, S., Gersdorff, N., Lange, K., and Roediger, M., Prospective evaluation of zirconia posterior fixed partial dentures: 7-year clinical results. *Int J Prosthodont*, 2013; 26: 164-71.
66. Roediger, M., Gersdorff, N., Huels, A., and Rinke, S., Prospective evaluation of zirconia posterior fixed partial dentures: Four-year clinical results. *Int J Prosthodont*, 2010; 23: 141-8.
67. Ruyter, I.E., Nilner, K., and Moller, B., Color stability of dental composite resin

References

- materials for crown and bridge veneers. *Dent Mater*, 1987; 3: 246-51.
68. Sabrah, A.H., Cook, N.B., Luangruangrong, P., Hara, A.T., and Bottino, M.C., Full-contour y-tzp ceramic surface roughness effect on synthetic hydroxyapatite wear. *Dent Mater*, 2013; 29: 666-73.
 69. Sailer, I., Feher, A., Filser, F., Gauckler, L.J., Luthy, H., and Hammerle, C.H., Five-year clinical results of zirconia frameworks for posterior fixed partial dentures. *Int J Prosthodont*, 2007; 20: 383-8.
 70. Sakagushi, R. and Power, J.M., *Craig's restorative dental materials*. Vol. 13. 2012: Saint Louis: Mosby.
 71. Sato, T. and Shimada, M., Transformation of yttria-doped tetragonal zro2 polycrystals by annealing in water. *J Am Ceram Soc*, 1985; 68: 356-9.
 72. Siarampi, E., Kontonasaki, E., Papadopoulou, L., Kantiranis, N., Zorba, T., Paraskevopoulos, K.M., and Koidis, P., Flexural strength and the probability of failure of cold isostatic pressed zirconia core ceramics. *J Prosthet Dent*, 2012; 108: 84-95.
 73. Sorensen, J.A., Kang, S.K., Torres, T.J., and Knode, H., In-ceram fixed partial dentures: Three-year clinical trial results. *J Calif Dent Assoc*, 1998; 26: 207-14.
 74. Spyropoulou, P.E., Giroux, E.C., Razzoog, M.E., and Duff, R.E., Translucency of shaded zirconia core material. *J Prosthet Dent*, 2011; 105: 304-7.
 75. Stawarczyk, B., Ozcan, M., Hallmann, L., Ender, A., Mehl, A., and Hammerlet, C.H., The effect of zirconia sintering temperature on flexural strength, grain size, and contrast ratio. *Clin Oral Investig*, 2013; 17: 269-74.
 76. Suttor, D., Bunke, K., Hoescheler, S., Hauptmann, H., and Hertlein, G., Lava--the system for all-ceramic zro2 crown and bridge frameworks. *Int J Comput Dent*, 2001; 4: 195-206.
 77. Swain, M.V., Grain-size dependence of toughness and transformability of 2mol% y-tzp ceramics. *J Mater Sci Lett*, 1986: 1159-62.
 78. Tinschert, J., Natt, G., Hassenpflug, S., and Spiekermann, H., Status of current cad/cam technology in dental medicine. *Int J Comput Dent*, 2004; 7: 25-45.
 79. Tinschert, J., Natt, G., Mautsch, W., Augthun, M., and Spiekermann, H., Fracture resistance of lithium disilicate-, alumina-, and zirconia-based three-unit fixed partial dentures: A laboratory study. *Int J Prosthodont*, 2001; 14: 231-8.
 80. Tinschert, J., Zwez, D., Marx, R., and Anusavice, K.J., Structural reliability of alumina-, feldspar-, leucite-, mica- and zirconia-based ceramics. *J Dent*, 2000; 28: 529-35.
 81. Toraya, H., Yoshimura, M., and Somiya, S., Calibration curve for quantitative analysis

References

- of the monoclinic-tetragonal zro₂ system by x-ray diffraction. *J. Am.Ceram. Soc*, 1984; 119-21.
82. Traini, T., Gherlone, E., Parabita, S.F., Caputi, S., and Piattelli, A., Fracture toughness and hardness of a y-tzp dental ceramic after mechanical surface treatments. *Clin Oral Investig*, 2014; 18: 707-14.
 83. Vagkopoulou, T., Koutayas, S.O., Koidis, P., and Strub, J.R., Zirconia in dentistry: Part 1. Discovering the nature of an upcoming bioceramic. *Eur J Esthet Dent*, 2009; 4: 130-51.
 84. Wagner, W.C. and Chu, T.M., Biaxial flexural strength and indentation fracture toughness of three new dental core ceramics. *J Prosthet Dent*, 1996; 76: 140-4.
 85. Wang, H., Aboushelib, M.N., and Feilzer, A.J., Strength influencing variables on cad/cam zirconia frameworks. *Dent Mater*, 2008; 24: 633-8.
 86. Wang, L., D'Alpino, P.H., Lopes, L.G., and Pereira, J.C., Mechanical properties of dental restorative materials: Relative contribution of laboratory tests. *J Appl Oral Sci*, 2003; 11: 162-7.
 87. Wennerberg, A., Ohlsson, R., Rosen, B.G., and Andersson, B., Characterizing three-dimensional topography of engineering and biomaterial surfaces by confocal laser scanning and stylus techniques. *Med Eng Phys*, 1996; 18: 548-56.
 88. Yilmaz, H., Aydin, C., and Gul, B.E., Flexural strength and fracture toughness of dental core ceramics. *J Prosthet Dent*, 2007; 98: 120-8.
 89. Zhang, F., Vanmeensel, K., Batuk, M., Hadermann, J., Inokoshi, M., Van Meerbeek, B., Naert, I., and Vleugels, J., Highly-translucent, strong and aging-resistant 3y-tzp ceramics for dental restoration by grain boundary segregation. *Acta Biomater*, 2015; 16: 215-22.
 90. Zhang, H., Kim, B.M., Morita, K., Hiraga, H.Y.K., and Sakka, Y., Effect of sintering temperature on optical properties and microstructure of translucent zirconia prepared by high-pressure spark plasma sintering. *STAM*, 2011; 12: 50-3.
 91. Zhang, Y., Making yttria-stabilized tetragonal zirconia translucent. *Dent Mater*, 2014; 30: 1195-203.
 92. Zhang, Y. and Kim, J.W., Graded structures for damage resistant and aesthetic all-ceramic restorations. *Dent Mater*, 2009; 25: 781-90.

Curriculum Vitae

PERSONAL INFORMATION

- Name: Kamal Khaled Ebeid Ahmed
- Telephone: +201006084044
- Address: 37, Andalus street, Heliopolis, Cairo, Egypt
- Email: kamal_ebeid@hotmail.com
- Date of Birth: 20/10/1987
- Place of birth: Egypt
- Nationality: Egyptian
- Marital status: Married

ACADEMIC BACKGROUND

- **2012-2014:** Master degree in Fixed Prosthodontics, Faculty of Dentistry, Ain Shams University, Egypt. (Excellent with honors)
- **2004-2009:** Bachelor degree of Dentistry, Faculty of Dentistry, Ain Shams University, Egypt (Excellent with honors)
- **2001-2004:** International General Certificate of Secondary Education “IGCSE” (105.4%)

WORK EXPERIENCE

- **2010-2011:** Demonstrator at Fixed Prosthodontics Department, Faculty of Dentistry, Future University, Egypt
- **2011-Present:** Demonstrator at Fixed Prosthodontics Department, Faculty of Dentistry, Ain Shams University, Egypt
- **2013-Present:** Guest Scientist Department of Prosthodontics, Propaedeutics and Dental Materials, Christian-Albrechts, University at Kiel, Germany

PUBLICATIONS

- K. Ebeid, S. Wille, A. Hamdy, T. Salah, A. El-Etreby, M. Kern: Effect of Changes in Sintering Parameters on Monolithic Zirconia Ceramic. J Dent Res; 93, Spec Iss A: 1444, 2014.
- K. Ebeid, S. Wille, A. Hamdy, T. Salah, A. El-Etreby, M. Kern. Effect of changes

in sintering parameters on monolithic translucent zirconia. Dent Mater; 2014;30:e419-424.

ADDITIONAL INFORMATION

- Former DAAD German Egyptian research short term scholarship (GERSS) holder.